

Excitation of acoustic-gravity waves in an isothermal atmosphere

By C. H. LIU and K. C. YEH, *Ionosphere Radio Laboratory, Department of Electrical Engineering, University of Illinois at Urbana-Champaign, Urbana, Illinois 61801*

(Manuscript received August 21, 1970, revised version November 30, 1970)

ABSTRACT

The excitation of acoustic-gravity waves in an isothermal atmosphere is considered in this paper. It is shown that the excitation due to mass production, momentum production and heat production can be discussed by examining the same differential equation. The sources are assumed to be extended and vary both in time and in space. Asymptotic methods are used to obtain analytic expressions for the radiation field for all times, from the arrival of precursors to any time thereafter. It is found that the transient response results from contributions from one, two or all three modes depending on the times from the arrival of precursors. The three modes are the high frequency acoustic mode, the intermediate frequency buoyancy mode and the low frequency gravity mode. Additional features of the transient behavior depend on the temporal as well as spatial variation of the sources. An example is given for which numerical computations are made. Possible applications of the results to geophysical problems are discussed and certain extensions of the results are proposed.

1. Introduction

There have been, of late, increasing interests in studying the generating mechanisms of acoustic gravity waves in the atmosphere. Early barometric observations showed that atmospheric waves were launched by the eruption of Krakata in 1883 and by the great Siberian meteor of 1908. Nuclear detonations in the atmosphere provided another generating mechanism. An outstanding example is the Soviet detonation of October 30, 1961 as it was followed by atmospheric and ionospheric perturbations on a worldwide scale (Dieminger & Kohl, 1962; Obayashi, 1962; Wickersham, 1966). The great Alaskan earthquake of March 23, 1964 generated waves observed in the ionosphere (Leonard & Barnes, 1965; Davis & Baker, 1965). The experimental evidence of Yuen et al. (1969) supports the thesis that atmospheric waves are excited by a coupling process with the traveling seismic waves. Auroral related atmospheric waves have also been detected. They are caused by either a supersonic displacement of auroral arcs (Wilson, 1969) or a sudden surge of electrojet currents following polar sub-

storms (Davis & da Rosa, 1969). More recently, it has been suggested that the cooling action resulting from the solar eclipse may generate bow shocks as the shadow of the moon is racing across the surface of the earth at a supersonic speed (Chimonas & Hines, 1970). For observers at temperate latitudes, a majority of observed waves cannot be identified as caused by these unusual conditions. Most investigators, therefore, turn to potentially important meteorological causes such as mountain waves, weather fronts, instabilities or distortions of jet streams, and severe storms. A certain type of waves with periods in the range 2-5 min has been found to be associated with severe tropospheric storms (Georges, 1968; Baker & Davies, 1969). There are also indications that weather fronts and jet streams may account for wave-like deformations in noctilucent clouds (Hines, 1968). This great variety of sources, both natural and artificial, has induced theoretical investigators to look into the relation between excitation mechanisms and the generation of waves. One of the earliest is Lamb who dealt with the subject in his well known book, *Hydrodynamics*. The problem of atmospheric

response to an impulse point source has been treated by Pierce (1963) and Row (1967). Especially successful is Row's theory in explaining ionospheric observations following a nuclear detonation and an earthquake. Dickinson (1969) in a very comprehensive work has studied the transient excitation of these waves by point impulses and switched-on sources. Certain authors have also used numerical approach to treat the problem. Using the wave number dispersion relation, Kato (1967) numerically studied the propagation of an impulse in the atmosphere. Donn & Shaw (1967) made numerical computations for the response of the model atmosphere due to large nuclear explosions. Mowbray & Rarity (1967) studied the transient impulses in an incompressible fluid model. Jones (1970) has also done some numerical computations using normal mode expansion.

Cole & Greifinger (1969) have carried out an asymptotic analysis for the case when the energy is released at a point on the ground. They found that the response of the atmosphere consists of at most three different frequency components. The higher frequency spherical acoustic front arrives at an observation point first. Some time later a cylindrical caustic at a lower frequency arrives and then splits into two frequencies. Thereafter, the response includes these three frequency components.

In this paper, the transient response of an isothermal atmosphere due to excitation is investigated again in a more general fashion. Instead of restricting ourselves to point, impulsive sources, we shall study the far field response due to sources of arbitrary spatial and temporal variation. The transient response is followed at all observation times. It is found that the general features of the response discussed by Cole & Greifinger (1969) for a point source are mostly retained but there are additional features which depend on the temporal as well as spatial behavior of the source.

The mathematical formulation is carried out in section 2. The approach is general and is capable of finding response due to various types of excitations by solving one differential equation. A method of solving for the far field transient response is discussed in section 3. It makes use of asymptotic techniques. As an illustration, an example is given in section IV for which the analytic expressions are derived and numerical results are computed and shown

as curves. In section V, certain applications of the results to geophysical problems are discussed and possible extensions to other cases are indicated.

2. Formulation

The atmosphere is assumed to be non-rotating and is made of stationary, inviscid ideal gas. The fluid equations of interest come from conservation laws and they are given by

$$\begin{aligned} \partial \rho / \partial t + \operatorname{div} \rho \mathbf{v} &= q_1 \\ \rho d\mathbf{v}/dt + \nabla p - \rho \mathbf{g} &= \mathbf{q}_2 \\ \rho^\gamma d(p\rho^{-\gamma})/dt &= (\gamma - 1)q_3 \end{aligned} \quad (1)$$

where q_1 , \mathbf{q}_2 and q_3 are respectively the rate of mass production per unit volume, the rate of momentum production per unit volume and the rate of heat production per unit volume. The source terms q_1 , \mathbf{q}_2 and q_3 are generally functions of time and space and are assumed to be localized so as not to modify the background atmosphere in a big way. For observers outside the source region, they can be treated as sources of waves as done by many investigators. The equilibrium atmosphere is assumed to be isothermal with an exponential distribution in pressure and density characterized by the scale height

$$H = kT/mg = c^2/\gamma g \quad (2)$$

Perturbations in the atmospheric variables are assumed to take place according to the scheme

$$\rho = \rho_0 + \rho', \quad p = p_0 + p', \quad \mathbf{v} = \mathbf{0} + \mathbf{v} \quad (3)$$

As seen from (3), the atmosphere is assumed stationary when unperturbed. The generalization to the case in which there is a background horizontal wind is straightforward at this stage. But it introduces complications later. When (3) is substituted into (1) and the resulting equations are linearized, a set of differential equations can be obtained. It is convenient to express the set in matrix form

$$\mathcal{D}\mathbf{F} = \mathbf{Q} \quad (4)$$

where the matrix operator is given by

$$\mathbf{D} = \begin{Bmatrix} \frac{\partial}{\partial t} & 0 & \frac{\partial}{\partial x} & \frac{\partial}{\partial y} & \frac{\partial}{\partial z} - (1/2H) \\ 0 & \frac{\partial}{\partial x} & \frac{\partial}{\partial t} & 0 & 0 \\ 0 & \frac{\partial}{\partial y} & 0 & \frac{\partial}{\partial t} & 0 \\ g & \frac{\partial}{\partial z} - (1/2H) & 0 & 0 & \frac{\partial}{\partial t} \\ -c^2 \frac{\partial}{\partial t} & \frac{\partial}{\partial t} & 0 & 0 & (\gamma - 1)g \end{Bmatrix} \quad (5a)$$

and the field vector and the source vector are respectively

$$\mathbf{F} = \begin{Bmatrix} \rho'/\rho_0^{\frac{1}{2}} \\ p'/\rho_0^{\frac{1}{2}} \\ v_x \rho_0^{\frac{1}{2}} \\ v_y \rho_0^{\frac{1}{2}} \\ v_z \rho_0^{\frac{1}{2}} \end{Bmatrix} \quad (5b) \quad \mathbf{Q} = \begin{Bmatrix} q_1/\rho_0^{\frac{1}{2}} \\ q_{2x}/\rho_0^{\frac{1}{2}} \\ q_{2y}/\rho_0^{\frac{1}{2}} \\ q_{2z}/\rho_0^{\frac{1}{2}} \\ (\gamma - 1)q_3/\rho_0^{\frac{1}{2}} \end{Bmatrix} \quad (5c)$$

The coordinate system is cartesian with z -axis pointed upward so that the constant gravity is given by $(0, 0, -g)$.

Let

$$\begin{aligned} D &= \det \mathbf{D} \\ \hat{\mathbf{D}} &= \text{adjoint of } \mathbf{D} \\ \hat{\mathbf{D}} \mathbf{Q} &= \mathbf{S} \end{aligned} \quad (6)$$

then (4) can be recast into

$$D\mathbf{F} = \mathbf{S} \quad (7)$$

The operator D is a scalar operator and is given by

$$\begin{aligned} D &= \frac{\partial^4}{\partial t^4} - c^2 \frac{\partial^2}{\partial t^2} \left(\frac{\partial^2}{\partial x^2} + \frac{\partial^2}{\partial y^2} + \frac{\partial^2}{\partial z^2} - \frac{1}{4H^2} \right) \\ &\quad - \omega_0^2 c^2 \left(\frac{\partial^2}{\partial x^2} + \frac{\partial^2}{\partial y^2} \right) \end{aligned} \quad (8)$$

The Brunt-Vaisala frequency is given by $\omega_0^2 = (\gamma - 1)g^2/c^2$. The operator D can be identified as the acoustic-gravity wave operator. For plane waves we may replace $\partial/\partial t$ by $-i\omega$ and $\partial/\partial x$ by ik_x , $\partial/\partial y$ by ik_y , and $\partial/\partial z$ by ik_z . Then $D = 0$ yields directly the dispersion relation of Hines (1960)

$$(k_x^2 + k_y^2)(1 - \omega_0^2/\omega^2) + k_z^2 = k_0^2(1 - \omega_0^2/\omega^2) \quad (9)$$

where $k_0 = \omega/c$ and the acoustic cutoff frequency $\omega_a = c/2H$. Our interest is to solve (7) for \mathbf{F} with the associated boundary or radiation condi-

tions. For convenience \mathbf{S} in (7) shall be called the equivalent source function. It is related to the true sources through an adjoint operation as given by the third equation of (6). Since \mathbf{Q} is assumed known, so is \mathbf{S} . Regardless of the type of source, our problem is reduced to solving the differential equation of the type (7) with a scalar acoustic-gravity wave operator given by (8). Methods are shown in the next section by which radiation fields of (7) can be obtained.

3. Far field transient response

The equation of concern is (7). We note that the differential operator D has constant coefficients and therefore the differential equation (7) can be conveniently solved by the transform method. The unknown field \mathbf{F} in the transformed domain can be found very easily since (7) becomes algebraic. The whole problem then depends on our ability to perform the inversion. It has been found that the exact inversion in wave propagation problems are very difficult in general. But if our interest is in the radiation field far away from the localized source, certain asymptotic methods can be used. These asymptotic methods also have the advantage of being interpreted in terms of ray optics and make the results physically meaningful.

The Fourier transform of (7) both in time and space reduces to

$$L(\mathbf{k}, \omega) \mathbf{F}(\mathbf{k}, \omega) = -\mathbf{S}(\mathbf{k}, \omega)/\omega^2 c^2 \quad (10)$$

where

$$L(\mathbf{k}, \omega) = (1 - \omega_0^2/\omega^2)(k_x^2 + k_y^2) + k_z^2 - (\omega^2 - \omega_a^2)/c^2 \quad (11)$$

and is related to the operator $D(\mathbf{k}, \omega)$ in (8) through $D = -\omega^2 c^2 L$. In the interest of not flooding this paper with too many symbols, a Fourier transform pair is denoted by the same symbol but distinguished by their arguments. For example, $\mathbf{F}(\mathbf{r}, \omega)$ is the Fourier transform in time of $\mathbf{F}(\mathbf{r}, t)$ and $\mathbf{F}(\mathbf{k}, \omega)$ is the Fourier transform in space of $\mathbf{F}(\mathbf{r}, \omega)$.

The transient response $\mathbf{F}(\mathbf{r}, t)$ is obtained by inverting $\mathbf{F}(\mathbf{k}, \omega)$ from (10). It is convenient to write the solution formally in the following form

$$\mathbf{F}(\mathbf{r}, t) = \frac{-1}{2\pi c^2} \int_{\Gamma} \omega^{-2} \mathbf{F}(\mathbf{r}, \omega) e^{-i\omega t} d\omega \quad (11)$$

where

$$\mathbf{f}(\mathbf{r}, \omega) = \frac{1}{(2\pi)^3} \int \frac{\mathbf{S}(\mathbf{k}, \omega)}{L(\mathbf{k}, \omega)} e^{i\mathbf{k} \cdot \mathbf{r}} d\mathbf{k} \quad (12)$$

The integration path Γ in (11) is parallel to the real ω -axis and above all singularities.

Lighthill (1960) has shown that, for (12), the far field approximation satisfying the radiation condition is given by

$$\mathbf{f}(\mathbf{r}, \omega) = \frac{1}{2\pi r} \sum_{\alpha} \frac{\mathbf{S}(k_{\alpha}, \omega)}{|\nabla_{\mathbf{k}} L|_{\mathbf{k}_{\alpha}} K^{\frac{1}{2}}} e^{i\mathbf{k}_{\alpha} \cdot \mathbf{r} + 0(r^{-2})} \quad (13)$$

where the summation is over the set of values of \mathbf{k} on the dispersion surface $L(\mathbf{k}, \omega) = 0$ in k -space, (i.e., the set of \mathbf{k} that satisfies the dispersion relation $L = 0$ or (9)) such that the normal to the surface at that point is in the direction of \mathbf{r} . Physically this indicates that the contribution to the radiation fields comes only from those rays whose group velocity vectors lie in the same direction as the observation point \mathbf{r} . The subscript α denotes the mode. It can be shown that for the case of interest there is just one mode for a given ω and henceforth we shall remove α . In (13), K is the Gaussian curvature of the dispersion surface and is given by

$$K(\mathbf{k}, \omega) = \frac{(1 - \omega_b^2/\omega^2)^2 [(1 - \omega_b^2/\omega^2)(k_x^2 + k_y^2) + k_z^2]}{[(1 - \omega_b^2/\omega^2)^2 (k_x^2 + k_y^2) + k_z^2]^2} \quad (14)$$

The detailed calculation of the various terms in (13) is carried out in the Appendix. It is found that for a given frequency ω , the ray that contributes to the far field at $\mathbf{r}(r, \theta, \phi)$ has a wave vector \mathbf{k} whose components must satisfy the following relations.

$$\begin{aligned} k_x^2 + k_y^2 &= \frac{\omega^2 - \omega_a^2}{c^2} \frac{\omega^4 \sin^2 \theta}{(\omega^2 - \omega_b^2)(\omega^2 - \omega_c^2)} \\ k_x^2 &= \frac{(\omega^2 - \omega_a^2)(\omega^2 - \omega_b^2) \cos^2 \theta}{c^2 (\omega^2 - \omega_c^2)} \\ k_y/k_x &= \tan \phi \end{aligned} \quad (15)$$

where $\omega_c = \omega_b \cos \theta$

The far field expression for \mathbf{f} in (13) can then be written as

$$\mathbf{f}(\mathbf{r}, \omega) = \frac{1}{4\pi r} \frac{\mathbf{S}[\mathbf{k}(\omega), \omega]}{\sqrt{(\omega^2 - \omega_b^2)(\omega^2 - \omega_c^2)}} e^{i r \xi(\omega)} \quad (16)$$

where

$$\xi(\omega) = \frac{1}{c} \sqrt{\frac{(\omega^2 - \omega_a^2)(\omega^2 - \omega_c^2)}{\omega^2 - \omega_b^2}} \quad (17)$$

and the dependence on \mathbf{k} of $\mathbf{S}(\mathbf{k}, \omega)$ is given by (15).

The expression (16) gives the radiation field at \mathbf{r} at a given frequency ω . It is interesting to note that even for the general source, as far as the spatial variation of the radiation field is concerned, it has the same behavior as the field due to a point source (Pierce, 1963). The difference is in the amplitude. From (16), we see that for a given ω , the amplitude of the radiation field is proportional to the components of the spatial spectrum of the equivalent source in the direction \mathbf{k} given by (15).

The transient response is obtained by substituting (16) into (11), yielding

$$\mathbf{F}(\mathbf{r}, t) = \frac{-1}{8\pi^2 c^3 r} \int_{\Gamma} \frac{\mathbf{S}[\mathbf{k}(\omega), \omega]}{\sqrt{(\omega^2 - \omega_b^2)(\omega^2 - \omega_c^2)}} e^{i r \xi(\omega)} d\omega \quad (18)$$

where

$$q(\omega) = r \xi(\omega) - \omega t \quad (19)$$

The exact inversion shown by (18) is difficult in general. In the following, the integral (18) will be evaluated asymptotically for large value of r by the method of saddle points. We note that for large r , the contribution to the integral comes mainly from the vicinity of saddle points ω , determined by

$$dq/d\omega = 0$$

or

$$\xi'(\omega_s) = t/r = 1/v_g(\omega_s) \quad (20)$$

A prime is used to denote differentiation with respect to the argument. v_g is the group velocity at which the wave packet propagates. The use of such asymptotic methods has been adequately reviewed by Felsen (1969). We shall apply these methods to our problem in the following. Interested readers may wish to consult this review for justifications of some steps.

Fig. 1 shows a plot of ξ as a function of ω . Only branches corresponding to propagating waves away from the source are shown. The curve is plotted for $\beta \equiv z/r = 0.1$ which corresponds to $\omega_c = 0.1 \omega_b$. Fig. 2 shows $\xi'c$ as a function of ω for a typical case. The saddle points are found by intersections of a parallel

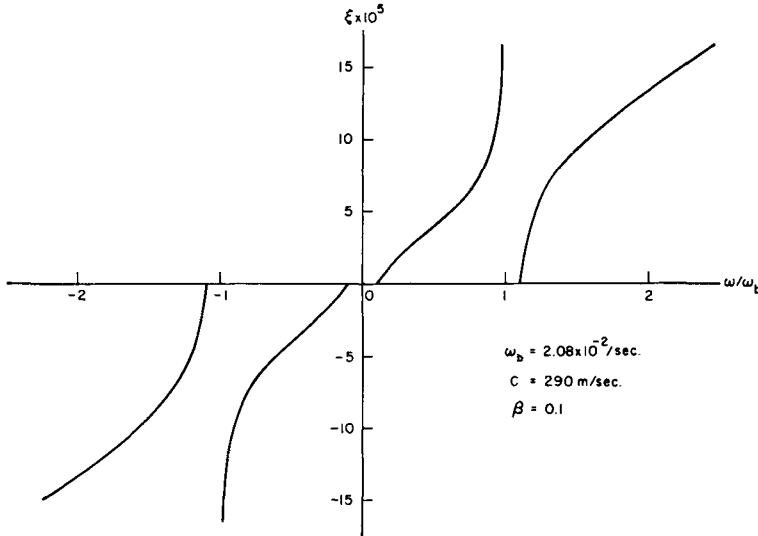


Fig. 1. A plot of ξ as a function of ω . Only portions of the curve that gives rise to the radiation fields are shown. $\omega_b = 2.08 \times 10^{-2} \text{ sec}^{-1}$, $c = 290 \text{ m/sec}$, $\beta = 0.1$.

line with these curves. The parallel line is drawn for a given $\tau = ct/r$. As many as three pairs of intersection points are possible, indicating contributions from three different frequencies. One is the high frequency and acoustic mode for $|\omega| > \omega_a$, and the other two are contributions from lower frequency bands, $\omega_0 < |\omega| < \omega_b$ and $\omega_c < |\omega| < \omega_0$. The former is called buoyancy mode and the latter gravity mode by some authors (Dickinson, 1969). The corresponding three pairs of saddle points are designated by ω_{s1} , ω_{s2} and ω_{s3} respectively. We note that in this construction, only real saddle points are located since only these contribute to the far field transient response. For a given observer (i.e. r is fixed), the parallel line as shown in Fig. 2 moves upward as t and hence also τ increase. In the following we shall derive asymptotic expressions of $F(\mathbf{r}, t)$ (18) in different regions of τ .

$\tau = ct/r < 1$. From Fig. 2 we see that there is no intersection hence no saddle point. The contour Γ in (18) is closed with a large semi-circle in the upper half-plane. Since there are no singularities inside the closed contour, we obtain

$$F_0(\mathbf{r}, t) = 0 \quad \text{if } t < r/c \quad (21)$$

This is in agreement with the principle of causality. The subscript 0 is used to indicate the response for this particular region.

$\tau = 1^+$. The saddle points at $\pm \omega_{s1}$ have very large magnitude. The contribution comes from very high frequencies. In this limit, we may make the following approximations in the integrand.

$$\xi(\omega) \approx \frac{\omega}{c} \left[1 - \frac{\omega_c^2 + \omega_a^2 - \omega_b^2}{2\omega^2} \right] \quad (22)$$

$$\frac{S[\mathbf{k}(\omega), \omega]}{\sqrt{(\omega^2 - \omega_b^2)(\omega^2 - \omega_c^2)}} \approx \mathbf{B} \left(\frac{\omega}{i} \right)^\alpha$$

where \mathbf{B} is a constant vector and α is a constant depending on the nature of the equivalent source function S .

Substituting (22) into (18), the integral can be carried out to yield, for $\alpha < 0$, say,

$$F_1(\mathbf{r}, t) \sim \frac{-1}{4\pi c^2 r} \mathbf{B} \left(\frac{\bar{r}}{a} \right)^{-(1+\alpha)/2} J_{-1-\alpha}(2\sqrt{a\bar{r}}) \quad (23)$$

$$a = \frac{r}{2c} (\omega_c^2 + \omega_a^2 - \omega_b^2), \quad \bar{r} = t - \frac{r}{c}$$

where $J_{-1-\alpha}(x)$ is the Bessel's function of the first kind of order $-(1+\alpha)$. For $\alpha \geq 0$, the integral can be evaluated in the similar manner (Felsen, 1969).

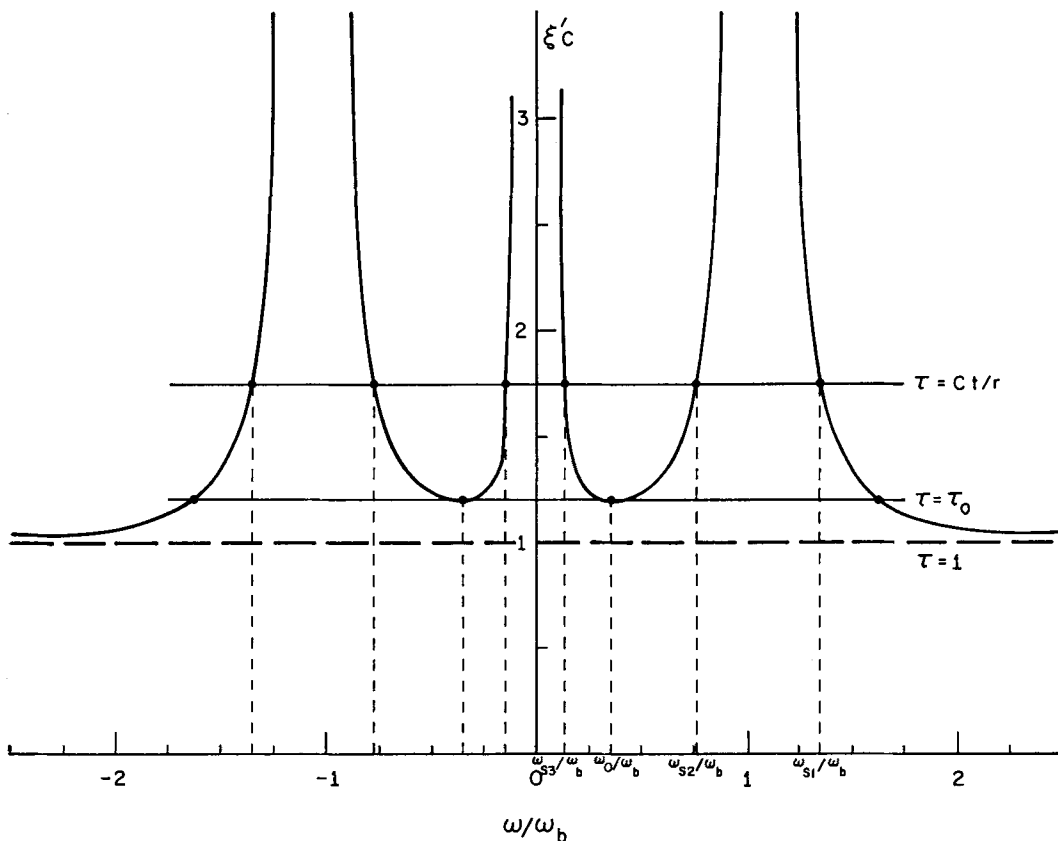


Fig. 2. A plot of $\xi'c$ as a function of ω/ω_b . Saddle points are given by the intersection of the curve with a horizontal straight line corresponding to a given τ .

$1 < \tau < \tau_0$. In this region contributions come only from $\pm\omega_{s1}$ corresponding to the acoustic mode (Fig. 2). The standard saddle point method gives

$$\begin{aligned}
 F_{II}(\mathbf{r}, t) \sim & \frac{1}{4\pi^2 c^2 r} \sqrt{\frac{2\pi}{r |\xi''(\omega_{s1})|}} \\
 & \times \left| \frac{S[\mathbf{k}(\omega_{s1}), \omega_{s1}]}{V(\omega_{s1}^2 - \omega_b^2)(\omega_{s1}^2 - \omega_c^2)} \right| \\
 & \times \cos [\xi(\omega_{s1})r - \omega_{s1}t - \pi/4 + \phi_1] \quad (24)
 \end{aligned}$$

where ϕ_i is the argument of

$$S[\mathbf{k}(\omega_{s1}), \omega_{s1}] / \sqrt{(\omega_{s1}^2 - \omega_b^2)(\omega_{s1}^2 - \omega_c^2)}.$$

$\tau = \tau_0$. When $\tau = \tau_0$, the saddle points ω_{s2} and ω_{s3} coalesce at ω_0 and similarly $-\omega_{s2}$ and $-\omega_{s3}$ at ω_0 . At $\pm\omega_0$, ξ'' vanishes and a higher order asymptotic expression must be used. From Fig. 2 we note that at ω_0 , ξ' has a local minimum

corresponding to a local maximum of the group velocity. The asymptotic expression is given by (see Bleistein, 1967)

$$\begin{aligned}
 F_{III}(\mathbf{r}, t) \sim & F_{II}(\mathbf{r}, t) + \frac{1}{\pi r} \left| \frac{S[\mathbf{k}(\omega_0), \omega_0]}{(\omega_0^2 - \omega_b^2)(\omega_0^2 - \omega_c^2)} \right| \\
 & \times \left[\frac{2}{|q'''(\omega_0)|} \right]^{\frac{1}{2}} A_t \left[\frac{q'(\omega_0)}{|q'''(\omega_0)/2|^{\frac{1}{2}}} \right] \\
 & \times \sin [\xi(\omega_0)r - \omega_0 t + \phi_0] \quad (25)
 \end{aligned}$$

where $A_t(x)$ is the Airy function. The first term on the right-hand side of (25) is the contribution from the acoustic mode and is given by (24). The second term indicates the contribution from the second order saddle point ω_0 . The Airy function can be physically interpreted as indicative of the initial build-up of the far field just prior to the time of arrival of the wave

packet with the local maximum group velocity and its subsequent decomposition into two distinct modes at frequencies ω_{s2} and ω_{s3} respectively. This situation is interpreted as the arrival of the caustic by Cole and Greifinger (1969).

$\tau > \tau_0$. Now all three pairs of saddle points are distinct. The transient response becomes

$$\begin{aligned}
 F_{IV}(\mathbf{r}, t) \sim F_{II}(\mathbf{r}, t) & \\
 + \frac{1}{4\pi^2 c^2 r} \sqrt{\frac{2\pi}{r |\xi''(\omega_{s2})|}} \left| \frac{S[\mathbf{k}(\omega_{s2}), \omega]}{\sqrt{(\omega_{s2}^2 - \omega_b^2)(\omega_{s2}^2 - \omega_c^2)}} \right| & \\
 \times \cos [\xi(\omega_{s2}) r - \omega_{s2} t + \pi/2 + \phi_2] & \\
 + \frac{1}{4\pi^2 c^2 r} \sqrt{\frac{2\pi}{r |\xi''(\omega_{s3})|}} \left| \frac{S[\mathbf{k}(\omega_{s3}), \omega_{s3}]}{\sqrt{(\omega_{s3}^2 - \omega_b^2)(\omega_{s3}^2 - \omega_c^2)}} \right| & \\
 \times \cos [\xi(\omega_{s3}) r - \omega_{s3} t + \phi_3] & \quad (26)
 \end{aligned}$$

The contribution comes from all three pairs of saddle points $\pm \omega_{s1}$, $\pm \omega_{s2}$ and $\pm \omega_{s3}$.

$\tau \gg \tau_0$. In this region, the three pairs of saddle points $\pm \omega_{s1}$, $\pm \omega_{s2}$ and $\pm \omega_{s3}$ are approaching the branch points $\pm \omega_a$, $\pm \omega_b$ and $\pm \omega_c$ of the integrand respectively (Fig. 2). A modified saddle point integration method must be applied for this case (Bleistein, 1967). The response now has contributions with frequencies ω_a , ω_b and ω_c respectively. The detailed expression of the transient response in this region depends on the explicit expression for $S[\mathbf{k}(\omega), \omega]$ and will be given for a special example in the next section. The explicit expression for S depends on the source models for various different physical situations.

Thus, we have derived the transient response of an unbounded isothermal atmosphere due to the excitation of general localized sources. We can now follow the response at an observation point \mathbf{r} far away from the source for all times. For $t < r/c$, there is no response. As $t \rightarrow r/c$, high frequency acoustic precursors first arrive. The frequency of this part of the response decreases as time increases until it approaches ω_a asymptotically. Sometime after the first arrival of the acoustic wave, a signal with frequency ω_b begins to build up corresponding to the arrival of the low frequency contribution. This portion of the response is decomposed into two components at frequencies ω_{s2} and ω_{s3} that eventually approach ω_b and ω_c respectively. Therefore after the arrival of this low frequency contribution,

the total response includes three components at frequencies ω_{s1} , ω_{s2} and ω_{s3} . The analytic expressions for the response at different times are given by (21) (23), (24), (25) and (26). In the text section, these formulae will be applied to the case of an impulsive point source.

In the derivation above we have assumed that $S[\mathbf{k}(\omega), \omega]$ does not introduce any additional singularities to the integrand in (18). If the contrary is the case, then some of the expressions given above may have to be modified. Depending not only on the temporal but also the spatial variation of the source, $S[\mathbf{k}(\omega), \omega]$ may introduce other branch points or poles in the integrand. The effects due to the presence of these additional singularities become important when either one of the saddle points approaches one of them. When this occurs, the response can be obtained by the modified saddle point method used above. If, in particular, the equivalent source $S[\mathbf{k}(\omega), \omega]$ has poles at $\pm \omega$, corresponding to, for instance, a turned on sinusoidal source of frequency ω_m , then the modified saddle point method will yield an expression for the response showing the buildup and arrival of the main signal as $\omega_s \rightarrow \omega_m$.

Finally we note that in our discussion we have implied that $S[\mathbf{k}(\omega), \omega]$ does not affect the saddle points of the integrand of (18). This is in general the case for localized stationary sources. For moving sources, this is no longer true. For this case the exponential function in the integrand of (18) will be modified and saddle points can be shifted (Lighthill, 1967).

4. An example

We now consider as an illustrative example the response of the atmosphere due to an impulsive point source. The response may be regarded as a Green's function or a propagator (Dickinson, 1969). For the sake of comparison, we take the model employed by Row (1967) who studied the response of the upper atmosphere to nuclear detonations. After Fourier transform in time, the Green's function satisfied the equation (Row, 1967)

$$\left(\frac{\partial^2}{\partial x^2} + \frac{\partial^2}{\partial y^2} + \frac{\omega^2}{\omega^2 - \omega_b^2} \frac{\partial^2}{\partial z^2} + \frac{\omega^2 (\omega^2 - \omega_a^2)}{c^2 (\omega^2 - \omega_b^2)} \right) \times G(\mathbf{r}, \omega) = -\delta(\mathbf{r}) \quad (27)$$

Fourier transform in space yields

$$L(\mathbf{k}, \omega) G(\mathbf{k}, \omega) = \left(1 - \frac{\omega_b^2}{\omega^2}\right) \quad (28)$$

where $L(\mathbf{k}, \omega)$ is given by (11). Eq. (28) may be regarded as one component of the vector equation (10) with $S(\mathbf{k}, \omega) = -c^2(\omega^2 - \omega_b)$. The results derived in the last section can be immediately applied to (28). We have, after some manipulations

$$G_0(\mathbf{r}, t) = 0 \quad t < r/c \quad (29)$$

$$G_I(\mathbf{r}, t) \sim \frac{1}{4\pi r} \left\{ \delta(t - r/c) - \sqrt{\frac{r(\omega_c^2 + \omega_a^2 - \omega_b^2)}{2c(t - r/c)}} \times J_1 \left[2\sqrt{(r/2c)(\omega_c^2 + \omega_a^2 - \omega_b^2)(t - r/c)} \right] \right\} \quad t \rightarrow r/c \quad (30)$$

$$G_{II}(\mathbf{r}, t) \sim \frac{1}{4\pi^2 r} \sqrt{\frac{2\pi}{r|\xi''(\omega_{a1})|}} |g(\omega_{a1})| \cos[\xi(\omega_{a1})r - \omega_{a1}t - \pi/4] \quad \frac{r}{c} < t < \frac{r}{c}\tau_0 \quad (31)$$

$$G_{III}(\mathbf{r}, t) \sim G_{II}(\mathbf{r}, t) + \frac{|g(\omega_0)|}{\pi r} \left[\frac{2}{|q'''(\omega_0)|} \right]^{\frac{1}{2}} \times A_1 \left[\frac{q'(\omega_0)}{|q'''(\omega_0)/2|} \right]^{\frac{1}{2}} \sin[\xi(\omega_0)r - \omega_0 t] \quad t \rightarrow \frac{r}{c}\tau_0 \quad (32)$$

$$G_{IV}(\mathbf{r}, t) \sim G_{II}(\mathbf{r}, t) + \frac{1}{4\pi^2 r} \sqrt{\frac{2\pi}{r|\xi''(\omega_{a2})|}} |g(\omega_{a2})| \cos[\xi(\omega_{a2})r - \omega_{a2}t + \pi/2] + \frac{1}{4\pi^2 r} \sqrt{\frac{2\pi}{r|\xi''(\omega_{a3})|}} |g(\omega_{a3})| \cos[\xi(\omega_{a3})r - \omega_{a3}t] \quad t > \frac{r}{c}\tau_0 \quad (33)$$

$$G_V(\mathbf{r}, t) \sim \frac{b_1}{2\sqrt{\pi}t^{\frac{3}{2}}} \sqrt{\frac{\omega_a^2 - \omega_b^2}{\omega_a^2 - \omega_c^2}} \cos\left(\frac{b_1^2 r^2}{4t} - \omega_a t - \frac{\pi}{4}\right) + \frac{(b_2 r/2)^{\frac{3}{2}}}{\pi\sqrt{6\pi}rt^{7/8}} \sqrt{\frac{\omega_b}{\omega_b^2 - \omega_c^2}} \cos\left[3t^{\frac{3}{2}}(b_2 r/2)^{\frac{3}{2}} - \omega_b t - \frac{\pi}{4}\right] + \frac{1}{4\pi r} \sqrt{\frac{2(\omega_b^2 - \omega_c^2)}{\pi\omega_c t}} \cos\left[\frac{b_3^2 r^2}{4t} - \omega_c t + \frac{\pi}{4}\right] \quad t \gg \frac{r}{c}\tau_0 \quad (34)$$

where

$$b_1 = \frac{1}{c} \sqrt{\frac{2(\omega_a(\omega_a^2 - \omega_c^2))}{\omega_a^2 - \omega_b^2}} \quad b_2 = \frac{1}{c} \sqrt{\frac{(\omega_b^2 - \omega_c^2)(\omega_a^2 - \omega_b^2)}{2\omega_b}} \quad b_3 = \frac{1}{c} \sqrt{\frac{2(\omega_a^2 - \omega_c^2)\omega_c}{\omega_b^2 - \omega_c^2}} \quad g(\omega) = \sqrt{\frac{\omega^2 - \omega_b^2}{\omega^2 - \omega_c^2}} \quad (35)$$

We note that the three terms in (34) are contributions from saddle points that are approaching $\pm\omega_a, \pm\omega_b$ and $\pm\omega_c$ respectively. The expression (34) is derived by the modified saddle point method which is valid when the saddle points are approaching the branch points of the integrand (Bleistein, 1967). Row (1967), assuming $\omega_c \ll \omega_b$, obtained an exact expression for the contribution from gravity mode in terms of Bessel's function of zeroth order (his eq. (12)). It is interesting to note that for $\tau = (ct/r) > 1$, the asymptotic expression of his result agrees exactly with the third term of (34). Of course he did not obtain contributions from acoustic mode (the first term of (34)) nor buoyancy oscillation (the second term of (34)) by virtue of his assumptions.

The expressions G_I to G_V for the response of the atmosphere due to an impulsive point source are plotted for certain typical sets of atmospheric parameters.

In Fig. 3, $\xi'c$ is plotted against the frequency

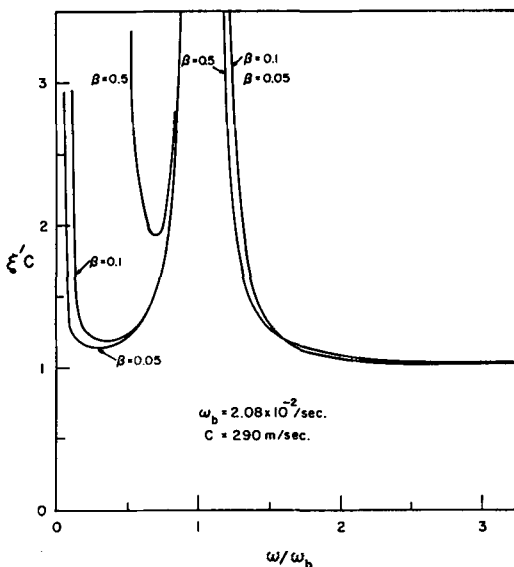


Fig. 3. $\xi'c$ vs. ω/ω_b for different values of $\beta = z/r$. $\omega_b = 2.08 \times 10^{-2} \text{ sec}^{-1}$, $c = 290 \text{ m/sec}$.

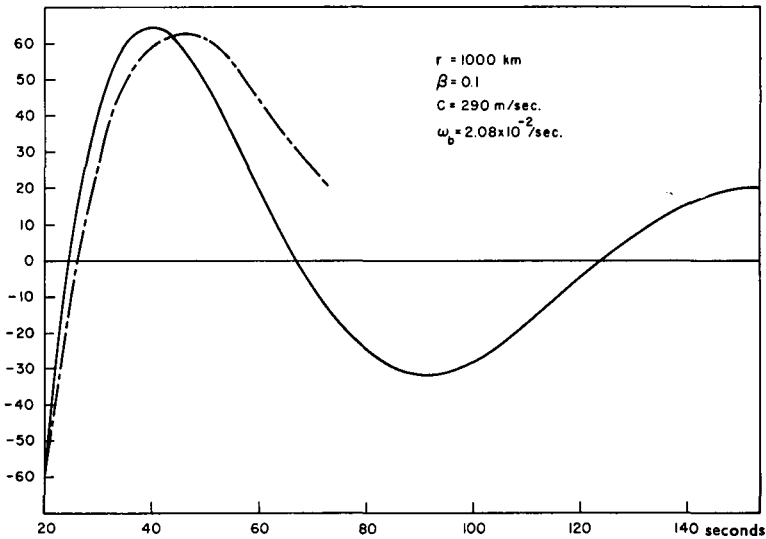


Fig. 4. The initial response of the atmosphere to an impulsive point source. The horizontal axis is time measured in $T - t_u$. The vertical axis is $G(r, t) \times (4\pi^2 r^{3/2})^{-1}$. The chained curve is computed from G_1 and it shows overlap with G_2 for small $T \cdot c = 290$ m/sec, $\omega_b = 2.08 \times 10^{-2}$ sec $^{-1}$, $r = 1\ 000$ km, $z = 100$ km.

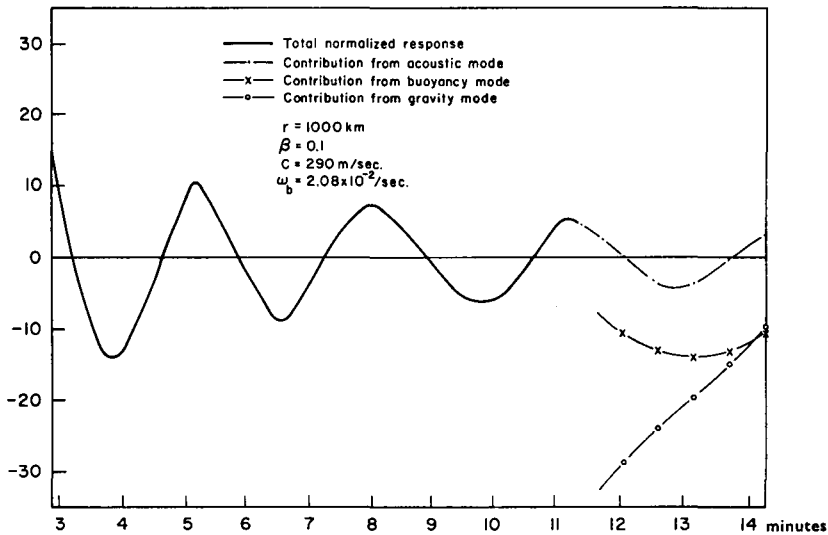


Fig. 5. Continuation of Fig. 4. The contribution to the response comes entirely from the acoustic mode for $T < 11.4$ min. Gravity mode and buoyancy mode begin to contribute at $T \approx 11.4$ min.

for different values of $\beta = z/r = \omega_c/\omega_b$ in an atmosphere with $c = 290$ m/sec and $H = 6.5$ km. The frequency is measured in $\omega_b = 2.08 \times 10^{-2}$ /sec and $\omega_a = 1.1 \omega_b$. Because of the symmetry, the curves are shown for positive ω only. These curves may then be used to find the saddle

points in the manner described in section III. In Figs. 4 through 7, normalized transient response are shown at an observation point 1 000 km away and 100 km above the source ($\beta = 0.1$) at various time intervals. The normalization factor is taken as $(4\pi^2 r^{3/2})^{-1}$. At $r =$

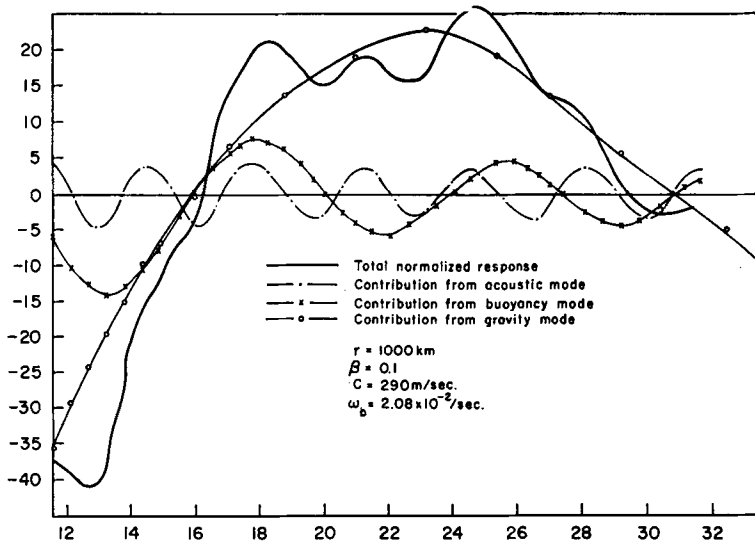


Fig. 6. Continuation of Fig. 5 showing contributions from all three modes.

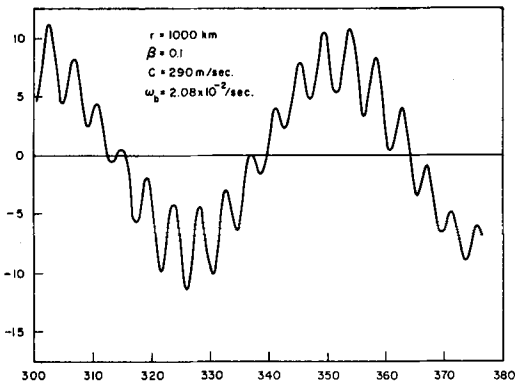


Fig. 7. Continuation of Fig. 6, but for very large time. The total response is essentially the gravity mode contribution modulated by the contribution from the acoustic mode.

1 000 km, the time of arrival for the acoustic front is $t = t_a = 3.45 \times 10$ sec. At $t = t_a$, the impulse arrives at the observation point. Fig. 4 shows the initial response of the atmosphere after the arrival of the front. The contribution is from the acoustic mode alone. The broken curve is G_I from (30) and the solid curve G_I from (31). There is a region of overlap in the time interval $15 \text{ sec} \leq t - t_a \leq 30 \text{ sec}$. It can be shown analytically that G_I and G_{II} reduce to the same expression in this region of overlap. Fig. 5

shows the response from the time interval $T \equiv t - t_a = 3 \text{ min}$ to $T = 14 \text{ min}$. For $T < 11.4 \text{ min}$ the response is still only acoustic. The oscillating period increases from the initial 100 sec to about 3.5 min. At $T = 11.4 \text{ min}$ ($\tau = \tau_0$), the contributions from the gravity and buoyancy modes come in. They are shown by broken curves in Fig. 5 together with the acoustic mode for $T > 11.4 \text{ min}$. The total response from this instant on includes all three frequency components and is obtained by adding the three individual contributions. This is done in Fig. 6 for $12 \text{ min} < T < 32 \text{ min}$. The total response as shown in Fig. 6 is very complex and its shape is changing with time since the relative magnitudes and frequencies of the three modes are changing. As time increases further, the frequencies of the acoustic, buoyancy and gravity modes approach ω_a , ω_b and ω_c respectively. The magnitude of the buoyancy oscillation becomes negligibly small and the dominant effect comes from the gravity mode. Fig. 7 shows the total response for $T > 300 \text{ min}$, some five hours after the arrival of the signal. The response is seen to be composed of a main oscillation with a period of approximately 50 min. Superimposed on this oscillation is a signal with a period of approximately 5 min. The former is the gravity mode and the latter is principally the acoustic mode.

For purposes of comparison, we take an

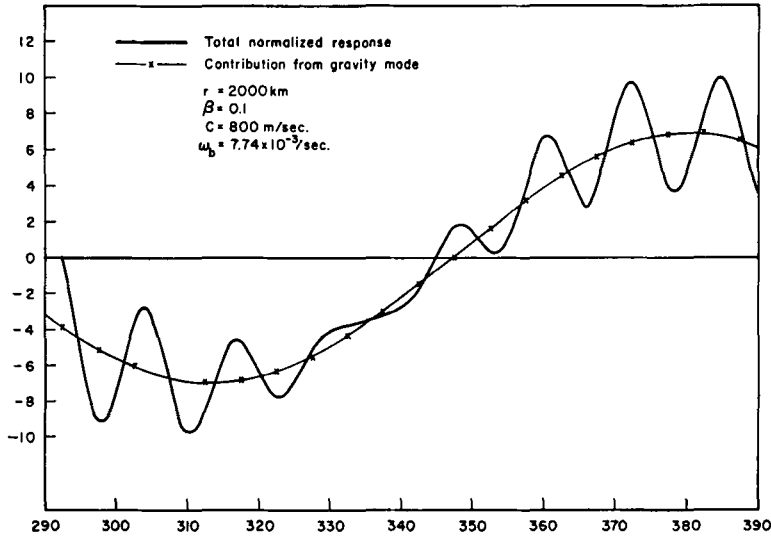


Fig. 8. The long time response of the atmosphere to an impulsive point source. $c = 800$ m/sec, $\omega_b = 7.74 \times 10^{-3}$ sec $^{-1}$, $r = 2\,000$ km, $z = 200$ km.

atmosphere with $c = 800$ m/sec and $\omega_b = 7.74 \times 10^{-3}$ sec $^{-1}$. The normalized response to an impulsive point source for large time T is shown in Fig. 8. The observation point is taken at $r = 2\,000$ km, $z = 200$ km so that β is still kept at 0.1. Again, the total response can be seen as the contribution from the gravity mode (period ≈ 2 hours) modulated by the acoustic mode (period ≈ 13 min).

5. Discussion

In this paper, the problem of excitation of acoustic-gravity waves in an isothermal atmosphere is investigated in a fairly general manner. Far field transient response of the atmosphere is derived for localized sources that vary arbitrarily in time and in space. Analytical expressions of the response are obtained for all times. It is found that the general behavior of the transient far field includes contributions from a high frequency component (acoustic mode) with $\omega > \omega_a$ and two lower frequency components with $\omega_a < \omega < \omega_b$ (buoyancy mode) and $\omega_c < \omega < \omega_a$ (gravity mode). The transient response depends on the temporal as well as spatial variation of the source.

Although no source models corresponding to physically realistic situations are discussed (an

example of discussions of this nature can be found in Pierce, 1968), our results are general enough to be applicable to the different types of sources that are thought to be responsible for many experimentally observed upper atmospheric disturbances. For example, the current experimental evidence associates production of certain infrasound and traveling disturbances in the ionosphere with auroral activities. There have been suggestions that the supersonic displacement of auroral arc may introduce an effective momentum source which can excite acoustic-gravity waves (Chimonas & Hines, 1970). An alternate candidate in wave excitation is the heating of the atmosphere by the auroral current. The relative effectiveness of both excitation mechanisms can be examined under the same frame of analysis as done in this paper. Also, the results may be applied to investigate the generation of acoustic-gravity waves due to severe weather system. Inside the storm region, nonlinear effects are very important. The nonlinear terms in the hydrodynamic equations may be taken to the right-hand side of the equations and treated as sources. The farfield response due to these sources may then be calculated by our formulae.

In our present discussion, the effect of the ground has not been taken into account. However, our results can be extended readily to

cover this case. The major modification will be the additional contributions from a reflected wave and a surface wave (Pierce, 1963). The surface wave is the well-known Lamb mode. The transient behavior of the reflected and surface waves may be evaluated in the same manner as is done in the calculation of (18).

Our discussion may be generalized so that the results will be applicable to the case of temperature-stratified atmosphere. In regions where geometric optics is valid, the transient response may still be written in the same form as in (18) with some modification in the integrand and the exponential function $q(\omega)$ replaced by the WKB form

$$q(\omega) = \int_z \xi(\omega, \eta) d\eta - \omega t \quad (36)$$

The asymptotic evaluation of $F(\mathbf{r}, t)$ can be carried out by the saddle point technique, leading to obvious modification in the results due to the change of character of $q(\omega)$.

Acknowledgment

This paper was prepared with the support of the National Aeronautics and Space Administration under grant NGR 14-005-002 and the Atmospheric Sciences Section of the National Science Foundation under grant GA 13723.

Appendix

In this Appendix, we shall calculate the various terms in (13). As seen from (11), the dispersion surface has an axial symmetry with respect to the k_z axis. In Fig. A.1, a cross-section of the surface $L(\mathbf{k}, \omega) = 0$ in the $k_x k_z$ plane is depicted. For a given ω , the surface has only one sheet. When $\omega > \omega_a$, the surface is an ellipsoidal surface of revolution and is closed. When $\omega < \omega_b$, the surface is a hyperbolic surface of revolution and is open. The former is commonly referred to as the acoustic branch and the latter the gravity branch. An example for each of these two branches are shown in Fig. A.1. For any wave vector \mathbf{k} on the dispersion surface, the unit normal to the surface is given by

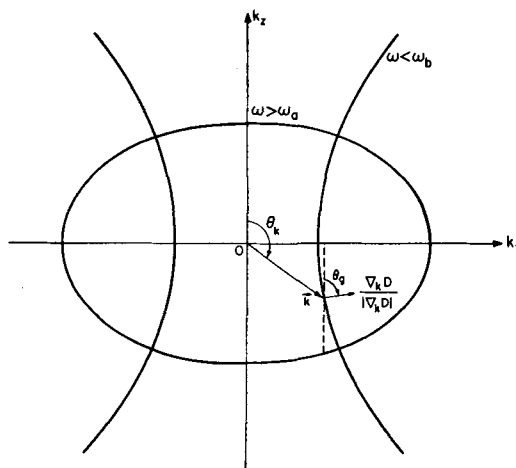


Fig. A.1. Dispersion surfaces for a typical acoustic wave ($\omega > \omega_a$) and a typical gravity wave ($\omega < \omega_b$).

$$\hat{n} = \frac{(\nabla_{\mathbf{k}} D)}{|\nabla_{\mathbf{k}} D|} \mathbf{k} = \frac{(1 - \omega_b^2/\omega^2) k_x \hat{x} + (1 - \omega_b^2/\omega^2) k_y \hat{y} + k_z \hat{z}}{\sqrt{(1 - \omega_b^2/\omega^2)^2 (k_x^2 + k_y^2) + k_z^2}} \quad (A.1)$$

The angle this normal makes with the k_z -axis is

$$\cos \theta_g = \hat{z} \cdot \hat{n} = \frac{k_z}{\sqrt{(1 - \omega_b^2/\omega^2)^2 (k_x^2 + k_y^2) + k_z^2}} \quad (A.2)$$

Therefore, if a normal is making an angle θ_g with the k_z -axis, k_x , k_y and k_z must satisfy

$$k_z^2 = (1 - \omega_b^2/\omega^2)^2 (k_x^2 + k_y^2) \cos^2 \theta_g / \sin^2 \theta_g \quad (A.3)$$

On the other hand, \mathbf{k} must also satisfy the dispersion relation in order to be on the dispersion surface. Substituting (A.3) into $L = 0$, (11), we obtain the following relation

$$k_x^2 + k_y^2 = \frac{(\omega^2 - \omega_a^2)}{c^2} \frac{\omega^4 \sin^2 \theta_g}{(\omega^2 - \omega_b^2) (\omega^2 - \omega_b^2 \cos^2 \theta_g)} \quad (A.4)$$

This gives the value of $k_x^2 + k_y^2$ for which the corresponding normal to the dispersing surface makes an angle θ_g with the k_z -axis. The corresponding k_z is obtained by substituting (A.4) into (A.3), yielding (Kato, 1967)

$$k_z^2 = \frac{(\omega^2 - \omega_a^2) (\omega^2 - \omega_b^2) \cos^2 \theta_g}{c^2 (\omega^2 - \omega_b^2 \cos^2 \theta_g)} \quad (A.5)$$

Let the angle between this wave vector and the z -axis be θ_k . Then θ_k satisfies

$$\cos \theta_k = \frac{k_z}{k} = \frac{(\omega^2 - \omega_b^2) \cos \theta_g}{\sqrt{\omega^4 - 2\omega^2 \omega_b^2 \cos^2 \theta_g + \omega_b^4 \cos^4 \theta_g}} \quad (\text{A.6})$$

It is easy to see from (A.6) that if $\theta < \pi/2$, θ_k is less than $\pi/2$ for the acoustic mode ($\omega > \omega_a$) and is greater than $\pi/2$ for the gravity mode ($\omega < \omega_b$).

We are now ready to evaluate (13). For an observer at the point $\mathbf{r}(r, \theta, \phi)$, the contributions come from those points on the dispersion surface whose normal is in the direction of \mathbf{r} . That is, we require

$$\theta_g = \theta, \text{ and } k_y/k_x = \tan \phi \quad (\text{A.7})$$

which together with (A.4), (A.5) and (A.6) determines the corresponding wave vector \mathbf{k}_α . From Fig. A.1, it is obvious that only one such

wave vector exist for a given ω . Hence we shall remove the subscript α on \mathbf{k} . Substituting (A.4) and (A.5) into (A.1) and (A.2), after some manipulation, we have

$$|\nabla_{\mathbf{k}} \mathcal{L}| K^{\frac{1}{2}} = \frac{2}{\omega^2} \sqrt{(\omega^2 - \omega_b^2)(\omega^2 - \omega_c^2)} \quad (\text{A.8})$$

where $\omega_c = \omega_b \cos \theta = \omega_b z/r$ has been used.

The exponential factor $\mathbf{k} \cdot \mathbf{r}$ can be computed in the following manner,

$$\begin{aligned} \mathbf{k} \cdot \mathbf{r} &= kr \cos(\theta_k - \theta) \\ &= kr [\cos \theta_k \cos \theta + \sin \theta_k \sin \theta] \\ &= \frac{r}{c} \sqrt{\frac{(\omega^2 - \omega_a^2)(\omega^2 - \omega_c^2)}{\omega^2 - \omega_b^2}} \\ &= r\xi(\omega) \end{aligned} \quad (\text{A.9})$$

Substituting (A.8) and (A.9) into (13), (16) is obtained.

REFERENCES

- Baker, D. M. & Davies, K. 1969. F2-region acoustic waves from severe weather. *J. Atmos. Terr. Phys.* 31, 1345-1352.
- Bleistein, Norman, 1967. Uniform asymptotic expansions of integrals with many nearby stationary points and algebraic singularities. *J. Math. and Mech.* 17, 533-560.
- Chimonas, G. & Hines, C. O. 1970. Atmospheric gravity waves induced by a solar eclipse. *J. Geophys. Res.* 75, 875.
- Chimonas, G. & Hines, C. O. 1970. Atmospheric gravity waves launched by auroral currents. *Planet. Space Sci.* 18, 565-582.
- Cole, J. D. & Greifinger, C. 1969. Acoustic-gravity waves from an energy source at the ground in an isothermal atmosphere. *J. Geophys. Res.* 74, 3693-3703.
- Davies, K. & Baker, D. M. 1965. Ionospheric effects observed around the time of the Alaskan earthquake of March 28, 1964. *J. Geophys. Res.* 70, 2251-2253.
- Davies, M. J. & da Rosa, A. V. 1969. Traveling ionospheric disturbances originating in the auroral oval during polar substorms. *J. Geophys. Res.* 74, 5721-5735.
- Dieminger, W. & Hohl, H. 1962. Effects of nuclear explosions on the ionosphere, *Nature* 193, 953-964.
- Dickinson, R. E. 1969. Propagators of atmospheric motions 1 and 2. *Rev. Geophys.* 7, 483-538.
- Donn, W. L. & Shaw, D. M. 1967. Exploring the atmosphere with nuclear explosions. *Rev. Geophys.* 5, 53-82.
- Felsen, L. B. 1969. Transients in dispersive media. *IEEE Trans. on Antenna and Propagation AP-17*, 191-200.
- Georges, T. M. 1969. HF Doppler studies of traveling ionospheric disturbances. *J. Atmos. Terr. Phys.* 30, 735-746.
- Hines, C. O. 1968. A possible source of waves in noctilucent clouds. *J. Atmos. Sci.* 25, 937-942.
- Hines, C. O. 1960. Internal atmospheric gravity waves at ionospheric heights. *Can. J. Phys.* 38, 1441-1481.
- Jones, W. L. 1970. A theory for quasi-periodic oscillations observed in the ionosphere. *J. Atmos. Terr. Phys.* 32, 1555-1566.
- Kato, S. 1967. The response of an unbounded atmosphere to point disturbances, 2, Impulsive disturbances. *Astrophys. J.* 144, 326-336.
- Leonard, R. S. & Barnes, R. A., Jr, 1965. Observation of ionospheric disturbances following the Alaskan earthquake. *J. Geophys. Res.* 70, 1250-1253.
- Lighthill, M. J. 1967. On waves generated in dispersive systems by traveling forcing effects, with applications to the dynamics of rotating fluids. *J. Fluid Mech.* 27, 725-752.
- Lighthill, M. J. 1960. Studies on magneto-hydrodynamic waves and other anisotropic wave motions. *Phil. Trans. Roy. Soc. (London), ser. A.* 252, 397-430.
- Mowbray, D. E. & Rarity, B. 1967. A theoretical and experimental investigation of the phase configuration of internal waves of small ampli-

- tude in a density stratified liquid. *J. Fluid Mech.*, 28, 1-16.
- Obayashi, T. 1962. Widespread ionospheric disturbances due to nuclear explosions during October 1961. Rept. Ionosphere Space Res., Japan, 16, 334-340.
- Pierce, A. D. 1963. Propagation of acoustic-gravity waves from a small source above the ground in an isothermal atmosphere. *J. Acoustical Soc. Am.* 35, 1798-1807.
- Pierce, A. D. 1968. Theoretical source models for the generation of acoustic-gravity waves by nuclear explosions. Symposium proceedings, Acoustic-gravity waves in the atmosphere. T. M. Georges. (Ed.), Supt. of Documents. U.S. Govt. Printing Office, Washington, D.C., 9-24.
- Row, R. V. 1967. Acoustic-gravity waves in the upper atmosphere due to a nuclear detonation and an earthquake. *J. Geophys. Res.* 72, 1599-1610.
- Wickersham, A. F. 1966. Identification of acoustic-gravity wave modes from ionospheric range-time observations. *J. Geophys. Res.* 71, 4551-4555.
- Wilson, C. R. 1969. Infrasonic waves from moving auroral electrojets. *Planetary and Space Sci.* 17, 1107-1120.
- Yuen, P. C., Weaver, P. F., Suzuka R. K. & Furumoto, A. S. 1969. Continuous, traveling coupling between seismic waves and the ionosphere evident in May, 1968 Japan earthquake data. *J. Geophys. Res.* 74, 2 256-2 264.

ВОЗБУЖДЕНИЕ АКУСТИКО-ГРАВИТАЦИОННЫХ ВОЛН В ИЗОТЕРМИЧЕСКОЙ АТМОСФЕРЕ

В статье рассматривается возбуждение акустико-гравитационных волн в изотермической атмосфере. Показано, что возбуждения благодаря производству массы, импульса и тепла может быть рассмотрено при исследовании одного и того же дифференциального уравнения. Источники предполагаются протяженными и меняющимися как во времени, так и в пространстве. Используются асимптотические методы для получения аналитических выражений излучаемого поля для всех времен, от прибытия предвестников до любого большего момента. Найдено, что переходная реакция атмосферных параметров складывается из одного, двух или всех трех типов колеба-

ний в зависимости от времени от момента прихода предвестников. Этими тремя типами колебаний являются высокочастотные акустические колебания, колебания благодаря архимедовым силам с промежуточной частотой и низкочастотные гравитационные колебания. Дополнительные особенности переходной реакции зависят от временных и пространственных изменений источников. Дан пример, для которого выполнены численные расчеты. Обсуждаются возможные применения результатов к геофизическим задачам и предлагаются определенные обобщения результатов.